Seasonality and Trends in Coastal Water Temperatures from NOAA Water Level Monitoring Stations along US Coasts

John A. Callahan[1,2*], Bailey Armos[1,3], Tigist Jima[1], Christopher Zervas[1]

[1]National Ocean Service, National Oceanic and Atmospheric Administration (NOAA), Silver Spring, Maryland, USA
[2]Ocean Associates, Inc., Arlington, VA, USA
[3]IBSS Corporation, Silver Spring, Maryland, USA

*****Corresponding Author
Email: john.callahan@noaa.gov
ORCID: https://orcid.org/0000-0002-6299-9388

Keywords: coastal hazards, water temperature, seasonal cycle, trends, extremes, marine heatwaves, tide gauges, monitoring

Abstract
Coastal regions are complex environments. They lie at the confluence of physical oceanic, atmospheric, and land-based processes, and continue to undergo significant change due to both natural and human-driven factors. Although it is well known that ocean sea surface temperatures (SSTs) have increased over the past several decades, extending these trends and patterns to coastal waters is nontrivial. We evaluated a new quality-controlled dataset of coastal water temperature collected at NOAA Center for Operational Oceanographic Products and Services (CO-OPS) water level monitoring stations. Water temperature (WT) records were analyzed at 95 stations extending from the mid-1990s to 2023 and representing all the major US coastal regions. Seasonal cycle metrics, linear trends, daily distributions, and extreme percentile thresholds were computed at each site. Seasonal cycles and peak times of year tracked well with solar heating and consistently tracked behind air temperature by a few days to a few weeks. US East Coast and Great Lakes regions have a much stronger seasonal cycle and larger range (up to 25°C) than West Coast and Island regions (as low as 3°C). The great majority of stations experience warming over this time period, with statistically significant trends at 56 of 95 stations, averaging approximately 0.5 °C/decade. Many of these locations are also experiencing sea level rise, most notably in the Southeast and Gulf regions. Although geographic patterns exist, variations are found in extreme threshold temperatures and trends station to station and between bay systems and the open coast, highlighting the need for continuous in situ monitoring along the coast. This study provides baseline statistics of long-term near shore coastal WT data and supports informed future planning and decision-making in this dynamic environment.

1 Introduction

Coastal regions are complex environments at the confluence of physical oceanic, atmospheric, and land-based processes as well as human-driven development, cultural, and economic activities. These regions have undergone significant change with increased stress in recent years due to sea level rise, changing storm patterns, and advancing human infrastructure, among others (May et al., 2023; Reimann et al., 2023, O'Donnell et al., 2024). Near-shore coastal waters are of critical importance as they are an indicator of the health of ecosystems, home to diverse vegetation and marine animal species, and support local business and economies (Liao et al., 2015; Trombetta et al., 2019; O'Donnell et al., 2024; Qu and Peng, 2023). Monitoring and extracting past trends in coastal regions is crucial to making informed future planning decisions in this dynamic environment. This paper aims to support these goals by introducing a new quality-controlled, continuously monitored, long-term coastal water temperature dataset along the US coasts.

It is well known that global ocean sea surface temperatures (SST) have been rising throughout the past century (Fox-Kemper et al., 2021) with increased warming in recent years (Samset et al., 2023; Terhaar et al., 2025; WMO, 2025). At global scales, a significant portion of long-term trends and interannual variation of sea surface height (SSH) can be directly attributable to the warming of ocean waters at the surface as well as at depths (Dangendorf, 2019; Fox-Kemper et al., 2021; Hamlington, 2020, 2024). Regionally, increased SST anomalies can affect currents and water density in the surface layer (Peña-Molino & Joyce, 2008), which may lead to higher sea levels along coast lines (Goddard et al., 2015; Ezer & Dangendorf, 2022). Monitoring ocean SST patterns over space and time is critical to understanding past behavior and feedback of Earth's climate system (Minnett et al., 2019; Global Climate Observing System, 2025). Although the measurement of SST originated from scientific interest in characterizing its spatial and temporal variations and understanding the relationship between SST, SSH, and ocean currents (Kennedy, 2014), extending trends and patterns of past ocean SSTs to coastal waters is nontrivial (Lima & Wethey, 2012; Ezer & Dangendorf, 2022).

Coastal water temperature is influenced by numerous local processes, such as solar heating; freshwater input from precipitation, run-off and rivers; land air temperature advection; adjacent vegetation and land-cover; and geochemical processes. Rising temperatures exacerbate water quality degradation by accelerating eutrophication (Malone and Newton, 2020), fueling the development of harmful algal blooms (Trombetta et al., 2019; Silva et al., 2025), and affect ocean marine life through deoxygenation and coral bleaching (Goreau & Hayes, 2024). Extreme coastal water temperatures also threaten fisheries by reducing overall catch potential (Cheung et al., 2021) and forcing significant habitat shifts for key species such as the American lobster and sea scallop (Tanaka et al., 2020) and Pacific salmon (Shelton et al., 2020).

Marine Heatwave (MHW) events in particular have been occurring more frequently (Androulidakis & Kourafalou 2022; Dong et al., 2025) and projected to further increase in the future throughout the world (Xu et al., 2022; Cooley et al., 2022; Zhang et al., 2026). These episodic extreme events further degrade coral reef structures (Neely et al., 2024; Ayad et al., 2025), enhance harmful algal blooms (Tester et al. 2010; Heal & Muni-Morgan, 2021), and negatively impact local flora and fauna (Neely et al. 2024; Hall et al., 2016).

Several past studies have looked at long-term behavior of coastal water temperature. However, several of these have used global or large scale datasets from satellite imagery or gridded model data and extracted data at the shore boundary (Lima and Wethey, 2012; Liao et al, 2015; Varela et al, 2023; GMRI, 2025). These data, albeit valuable for offshore ocean behavior, are unable to capture

the highly localized behavior of the waters adjacent to land. Other studies had small spatial extents using small scale coastal buoys, stationary monitoring sites, or small scale satellite imagery (Seekell and Pacea, 2011; Bashevkin et al., 2022; Hinson et al., 2022, other refs). There are few observational datasets on climate time scales of very near shore, shallow coastal water temperature.

The National Ocean Service's (NOS) Center for Operational Oceanographic Products and Services (CO-OPS), the US agency responsible for collecting and distributing observations and predictions of water levels and currents, monitors water temperature at many of their water level monitoring stations (Miller and Luscher, 2018; Armos et al., 2025; Dusek et al., 2024). A core purpose of CO-OPS data collections is to ensure the health and safety of US citizens, its economy, and its natural resources. These stations are well established and operate continuously, making them ideal for monitoring the very shallow waters and the influence of land surface vs open ocean. CO-OPS stations are point locations installed on land and can serve as a nearly independent *in situ* data source from gridded model reanalysis and satellite altimetry driven SST datasets.

There is an extremely tight connection between the health and condition of the ocean, particularly in coastal areas and major lakes, and human health, safety, and economic prosperity (Bailey et al., 2019). We address the concern of sparse availability of quality-controlled shallow coastal water temperature observations by evaluating the historical water temperature data collected at the NOAA CO-OPS stations along US coasts. Armos et al (2025) recently reviewed past water temperature monitoring methods at CO-OPS and performed several QC procedures to remove poor quality data. Their work identified numerous stations whose data records may be appropriate for describing past patterns and trends of water temperature along the near coast. The current study takes the next step and evaluates several metrics on the historical water temperature data records. The primary objectives of these efforts are to establish this new dataset as a viable option for long time scale studies, to provide baseline statistics of the historical metrics, and to assess the consistency and quality of the results.

This paper is organized in the following way. The geographic distribution of CO-OPS stations and a description of their data records are first provided, followed by a description of the statistical methods. Results are then reviewed, divided into three components: seasonality, daily distributions, and linear trends. Seasonal climatologies are generated at each station and compared to long term average air temperature and mean sea level. Empirical distributions of daily mean WT are generated and used to estimate extreme WT likelihood amounts. Linear trends are developed for each station over all years and months, for each month individually (e.g., Jan trend, Feb trend, etc…), and for the annual minimum, maximum, and range. Lastly, the WT data generated in this study are applied to two use cases: 1) the station point-based WT trends are compared against the well-known, globally gridded NOAA Optimally Interpolated Sea Surface Temperature (OISST) dataset in North Carolina, and 2) the frequency and duration of marine heatwave are evaluated for Key West, FL.

2 Data Sources and Station Locations

2.1 Water temperature data and station selection

Although the primary purpose of NOAA CO-OPS monitoring stations is for collection of water levels and currents, many of these stations are equipped to also monitor additional environmental conditions. This is intended to maximize public benefit of observation platforms and includes meteorological factors that directly affect inundation over short periods of time (e.g., air temperature, wind speed and direction, barometric pressure) as well as water temperature and conductivity providing a measure of the water's salinity concentration and are directly related to water density,

vertical turbulence/mixing, water quality, and ecological health (Miller and Luscher, 2018, Dusek *et a*l, 2024). Water temperature measurements began to be broadly integrated into CO-OPS monitoring protocols in the mid-1990s (Edwing 1991).

The current study uses the quality controlled output from Armos et al. (2025). In that report, they evaluated the historical water temperature data records across CO-OPS monitoring station network and described the instruments, monitoring protocols, and operational real-time quality control checks. Most WT sensors are thermistors attached near the end of the water level monitoring infrastructure, e.g, at the end of acoustic PVC tubes. Starting in the early 2000s, CO-OPS also began to deploy water conductivity sensors at a few select stations, which also concurrently measure temperature. Several stations included a secondary water temperature sensor allowing for one to one comparisons at select stations during overlap periods. Since there was no standard depth placement for water temperature monitoring, sensor depth may have changed over time at some stations, e.g., after station maintenance or upgrades. However, all measurements were near the surface, with approximately 95% of current deployments within 4 m of MLLW, and 80% of sensor depth changes were within 2 meters. Sensor depth changes greater than 0.5 m were investigated further and stations with significantly different data before and after the depth change were marked as incomplete and not used for this study.

As part of their data QC producers, Armos *et al*. (2025) computed daily mean water temperature throughout each station's POR, requiring at least 50% of hourly records availability for each day. Out of the 220 stations evaluated (as of December 2024), 174 stations met the NWLON requirement of a minimum of 19 years of continuous operation (Dusek et al. 2024). A multitiered quality control (QC) set of procedures were applied to each of these stations' period of record (POR), removing erroneous or poor quality observations. After the QC procedures were performed, 49 (28%) of station data records were deemed insufficient for use in longer term studies. This included stations that had large or frequent data gaps, unexplained extended sensor drifts or extended discontinuities in the data, or shifts in data due to abrupt changes of the depth of the water level sensor. QC procedures included both automated and manual methods, including comparing each station's time series with surrounding neighbors.

The current study evaluated the remaining 125 stations with cleaned WT data records from Armos *et al* (2025). We identified 95 stations that had observations spanning at least 20 years, did not have significant gaps near the beginning or end of the POR, and did not include heating elements in locations where ice buildup frequently occurs, such as in the Great Lakes region. Daily mean WT data records for the 95 stations served as the basis for the current study's statistical analysis and are summarized below.

Stations were classified and represented all of the major geographic regions of the US (Figure 1; Figures S1-S4), including the US East Coast (Northeast and Southeast regions), Gulf Coast (Eastern and Western Gulf regions), West Coast (Northwest and Southwest regions), Great Lakes, Alaska, Caribbean Islands, and the Pacific Ocean Islands. Local environments of the stations are chosen to limit the influence of waves and external influences, such as boat traffic or human infrastructure (ref). However, natural landscapes around each station are widely varied, for example, along open coasts, within small and large ocean bays and sounds, up tributaries, behind barrier islands, among other similar environments. Location metadata for each station and finer scale maps are provided in the Supp Materials.

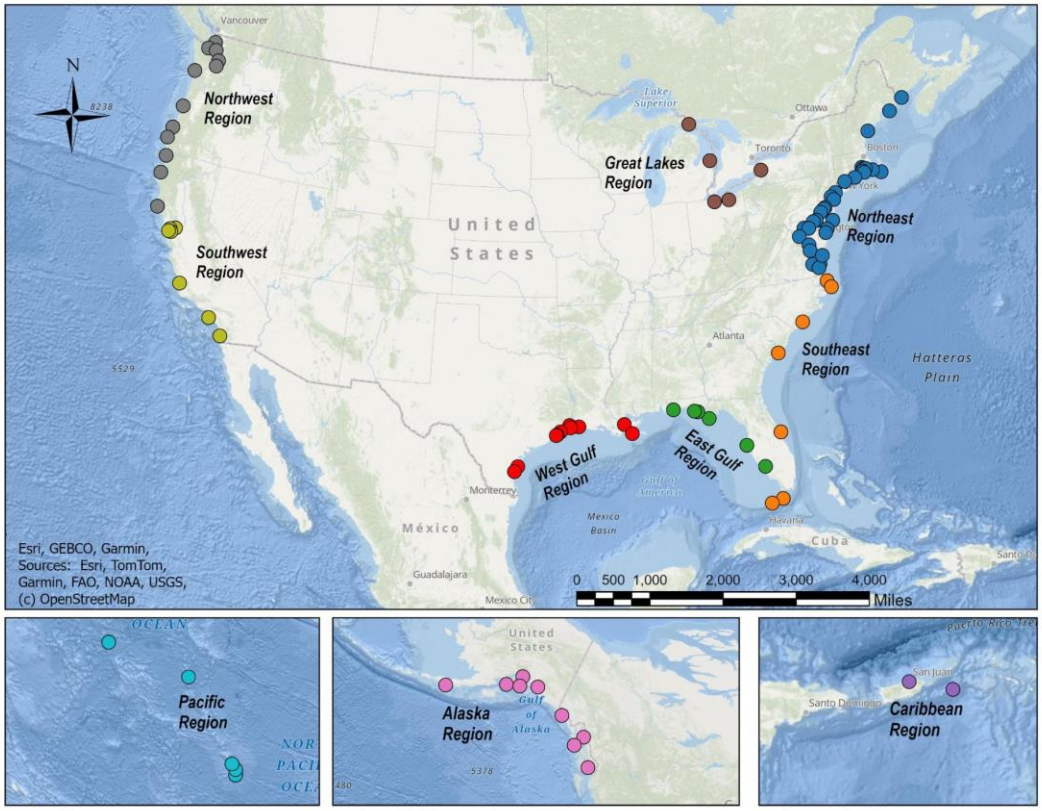

Figure 1. Map of all stations (N = 95) and geographic regions used in this study. Finer scale regional maps supplied in Figures S1-S4 in the Supplemental Materials.

The regions with the most and least stations were the Northeast (32) and Caribbean Islands (2) with all other regions ranging from 5 to 12 stations per region (Table 1). The number of days with daily mean WT within each station's POR ranged from 5,559 days (15.2 years) at Port Arthur, TX to 10,788 days (29.5 years) at Friday Harbor, WA. The Great Lakes and the Western Gulf regions had the most recent (9/22/2003 and 9/13/2000, respectively) and shortest mean PORs (19.54 and 19.30 years, respectively). Region mean PORs were predominantly between 23 - 27 years in length with completeness percentages from 84-96%.

Table 1. Summary of station historical water temperature records per geographic region used in this study. Individual station data inventory statistics are found in Figure S5 in Supplemental Materials.

Region	Number of Stations	Start Year	Record Length (years)	Completeness (percent)
Northeast	32	4/27/1997	24.34	91.38
Southeast	7	1/7/1996	24.09	86.50
East Gulf	6	1/9/1996	24.67	88.81
West Gulf	10	9/13/2000	19.30	88.42
Caribbean	2	2/14/1995	22.91	83.90
Great Lakes	5	9/22/2003	19.54	96.45

Alaska	9	9/13/1994	26.71	91.48
Northwest	12	11/6/1993	27.38	92.06
Southwest	7	12/18/1993	27.52	92.06
Pacific Islands	5	2/15/1994	26.53	88.80

2.2 Air temperature and water level station data records

Hourly observations and monthly mean sea levels (computed from hourly data) over each station's POR were obtained through the CO-OPS Data API[1]. Only accepted monthly mean sea levels (MSL) were used in the current study, i.e., preliminary data are not included. As stations were primarily intended for water level monitoring, record lengths for MSL data are generally equal or longer than that of WT data. Exceptions to this are three stations located in southwest TX (Port Arthur, Rollover Pass, and Baffin Bay) where although preliminary water levels are available since the beginning of the station POR, accepted verified MSL records do not begin until the early 2010s.

Air temperature (AT) data, measured approximately 1.2 - 2.0 meters above the land surface, were acquired for each station (Edwing, 1991; NWS, 2023). Consistent with water temperature and water level protocols, hourly observations of AT were used to generate daily mean values and daily climatologies, and automated QC procedures were applied to remove erroneous observations. Generally, AT records exhibited a level of completeness comparable to that of water temperature with less frequent data gaps. However, temporal coverage differed; while water temperature collection began on average in mid-1997, air temperature monitoring did not commence until approximately over five years later. The air temperature dataset used in this study concludes in 2022, following QC procedures performed by CO-OPS described in Armos et al. (2025).

3 Methods

Daily mean water temperature data from Armos et al (2025) are used as input to the current study. Monthly mean WT was computed throughout the station POR and required at least 50% (~ 15 days) of daily mean values for each month. Daily and monthly climatologies were generated for each station requiring at least 10 years worth of accepted mean values. Three separate main types of metrics were then investigated: 1) seasonality, 2) daily distributions and associated extreme thresholds, and 3) linear trends, and two types of application case studies, 1) comparing linear trends at stations to OISST gridded dataset in North Carolina, and 2) computing marine heatwave frequency in Key West, FL.

3.1 Seasonality

We assessed the seasonality of coastal water temperature by first computing the daily climatologies, as the simple average daily mean WT for each calendar day over each station's POR. The mean annual range was computed by subtracting the minimum from maximum value from the daily climatology. Daily climatologies and mean annual ranges were also computed for air temperature at each station and compared through correlation analysis. Pearson product-moment correlation coefficients between water and air temperature were computed for lags of up to 120 days in each

[1] https://tidesandcurrents.noaa.gov/api-helper/url-generator.html

direction. Negative lags represent when air temperatures precede water temperature and positive lags represent the reverse. The lag (in days) that resulted in the largest correlation at each station was identified.

Monthly climatologies were also generated, computed in the following fashion:

$$WTclim_j = \sum_{i=1}^{N} WTmon_{i,j} - WTclim_{mean} \qquad \text{(Equation 1)}$$

where $WTclim_j$ is the water temperature monthly climatology for month j (from 1 to 12), $WTmon_{i,j}$ is the mean monthly WT, i represents each year (ranging from 1 to the end of the POR), N is the number of years, and $WTclim_{mean}$ is the mean water temperature over all months in the entire POR, i.e., the climatological mean. Subtracting the climatological mean WT from each month is analogous to CO-OPS' typical monthly mean sea level processing relative to each station's official Mean Sea Level datum. Months with the climatological monthly maximum WT and MSL were found, noting the number of months lag and direction. Negative (positive) lags represent when peak mean sea levels precede (succeed) peak water temperatures.

3.2 Daily Distributions and Extremes

Distributions of daily mean water temperature were generated for each station over its POR using a Gaussian Kernel Density Estimator (KDE) with the bandwidth (i.e., smoothing factor) automatically determined using the default Scott's method (Silverman, 1986; Scot, 1992). Plots and basic descriptive statistics were generated to characterize the shapes of the distributions and compare between stations and geographic regions. Statistics included the mean, median, standard variation, skewness, and kurtosis. Estimates of the daily extremes at 90, 95, 99% likelihoods were generated from the empirical KDE-based distribution. The 90th percentile was chosen as it's commonly used as a marine heatwave threshold; likewise, the 95th and 99th percentiles were chosen as they are often used to generate exceedance probability statistics in extreme value analysis.

3.3 Linear Trends

Linear trends were computed for each station using the monthly anomalies, i.e., each month's mean temperature minus its monthly climatology. Linear trends, rather than high polynomials or other formulations, were chosen to align with CO-OPS philosophy of providing easily interpretable metrics of long-term past environmental changes as part of its publicly available products, such as monitoring long term changes in local sea level rise (Zervas, 2009). No attempt was made to identify acceleration or the decomposition into additional frequencies. Before an appropriate linear model could be constructed, the existence of serial correlation and seasonality were evaluated.

Autocorrelation and partial autocorrelation plots on the monthly anomalies were generated for each station at lags up to 24 months (see Figures S15 and S16 in the Supplemental Materials). The monthly autocorrelation is largest at one month lag and decreases gradually whereas the partial autocorrelation sharply cuts off after one month. These plots as well as the Ljung-Box and Durbin-Watson tests (not shown) demonstrate strong serial correlation at one month lag. Additionally, inspection of the monthly time series and the seasonality plots (see Section 4.1) indicate water temperatures experience strong seasonality across nearly all locations.

Based on these results, an Autoregressive Integrated Moving Average (ARIMA) with a lag of one month model, notated as ARIMA(1,0,0), has been chosen to compute linear trends. ARIMA models simultaneously decompose the time series into linear and seasonal components, account for serial autocorrelation, and optimize parameters using maximum likelihood estimation. Seasonality was accounted for through the use of 12 exogenous variables representing each month, resulting in separate weights for each month analogous to long-term monthly climatology. This methodology is identical to what is used by CO-OPS for its official sea level change trend rates (Zervas, 2009). The model is structured as follows:

$$WTmon_i = m\,t_i + w_j + \rho_1(WTmon_{i-1} - m\,t_{i-1} - w_{i-1}) + \in_i \qquad \text{(Equation 2)}$$

where $WTmon_i$ is the monthly mean temperature and t_i is the month, both running from 1 to the end of the station POR, w_j is the weight for month j (j ranges from 1 to 12), ρ_1 represents the lag one-month autoregressive coefficient, and *i* represents the monthly residual. Note the autoregressive factor is multiplied to the previous month's anomaly. The value of m, the slope of the trend line, is accepted as the linear trend rate. The 90% confidence interval around each trend rate was determined by multiplying the standard errors by 1.645, assuming a Normal distribution of errors. As well, the Augmented Dickey-Fuller and Durbin-Watson statistical tests were run to test for stationarity and the presence of serial correlation (at the 90% confidence level) in the monthly residual time series, respectively. Mean trends were then computed across each geographic region. For comparison, trends in relative mean sea level were computed at each station using an identical method over the years 1992 to 2023, spanning the length of all water temperature records.

Linear trends were also computed for annual minimum, annual maximum, and annual range as well as for each month at each station. Annual minimum and maximum values were derived from the daily mean WT data for that year, and the range is simply the difference between them. Only years with at least 85% of daily data were included. For monthly trends, all data for each month (i.e., all Jans, Febs, …) over each station's period of records were used in the trend computation. Depending on the station and data gaps present, each month may have a different number of data points but always less than the POR number of years. A basic least squares linear regression (non-ARIMA) was used to compute the slope of the trend line as seasonality and aerial correlation were not as strong on interannual time steps.

3.4 Application Case Studies

Lastly, water temperature data generated here are employed in two different example use cases in North Carolina and South Florida. In North Carolina, we compare linear trends at stations to linear trends found in the globally gridded NOAA OISST dataset, a blend of satellite, ship, and buoy measurements processed independently of CO-OPS station observations. The nearest grid cell following along the path of the local water body (i.e., not crossing land) in the OISST grid was chosen for the comparison. Linear trends for the OISST data were computed over 1992 to 2023 using the ARIMA(1,0,0) model, the same station-based method described in Section 3.3. This process was performed for all stations in this study. (Note that seven stations located within larger systems, namely Bergen Point, NY; Newbold, PA; Burlington, NJ; Philadelphia, PA; Washington, D.C.; Bayou Gauche, LA; and Juneau, AK, were over 100 km away from the nearest appropriate OISST grid cell and were not included.) Large differences were noted and investigated at two NC stations.

Second, the frequency and duration of high temperature anomalies and their accumulated heat stress were computed at Key West, FL (8724580). We follow the simple generally accepted definition of a Marine Heatwave (MHW), currently in use through the NOAA National Marine Ecosystem Status

application (NAMES, 2026), as an event when the daily mean water temperature exceeded the overall 90th percentile of the historical record for at least five consecutive days. We calculated the number of events per year and the maximum duration of events per year.

4 Results

4.1 Seasonality

Strong seasonal patterns of monthly anomalies are observed at nearly all stations (Figure 2) with peak temperatures in July and August and minimum temperatures in January and February. As expected, WT at stations in the typically warmer climates (e.g., reaching 25-30 ℃ during the summer in the Gulf Coasts and Pacific Islands) are higher than stations in the colder climates (e.g., dropping to less than 5 ℃ in the winter in Great Lakes and Alaska). The color gradients in Figure 2 represent the strength of the cycle and not absolute water temperature as the values are relative to each station's climatological mean. (Figure S7 in the Supplemental Materials displays the same seasonal patterns of absolute temperature rather than relative.)

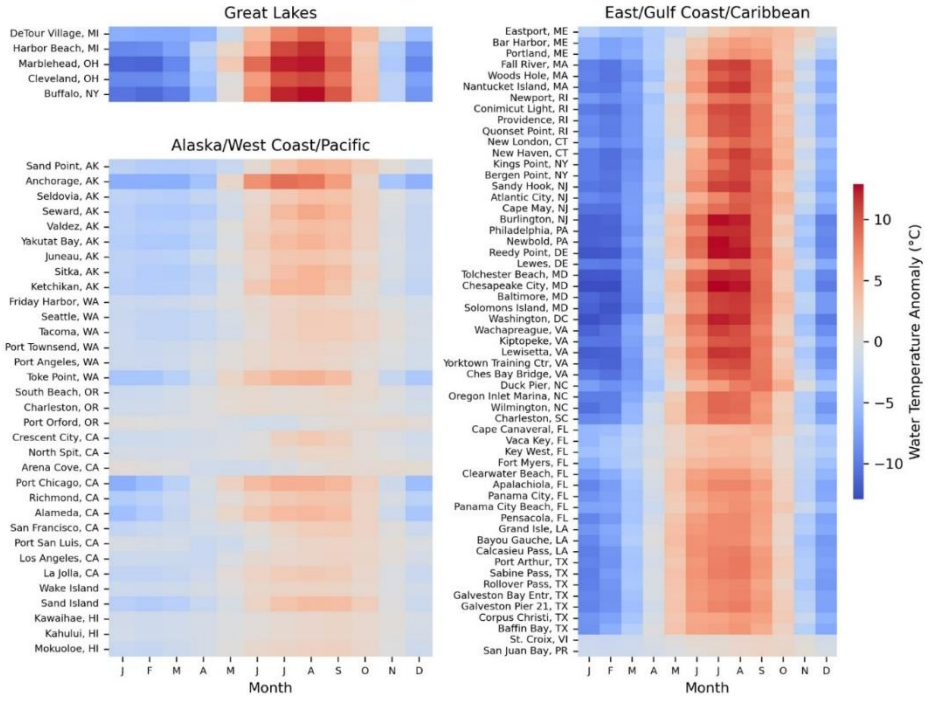

Figure 2. Mean seasonal cycle of coastal water temperature. Monthly mean values are in ℃ relative 952 to each station's climatological mean temperature.

In general, stronger seasonal cycles are found at stations on the East and Gulf Coasts than on the West Coast, and in northern areas than southern areas. Stations in the Great Lakes and Mid-Atlantic regions show the strongest seasonal patterns with monthly climatological variations up to 12 ℃ from the station long-term mean. Likewise, daily climatologies for sample stations from each region are presented in Figure 3. Blue and red curves represent WT and AT, respectively.

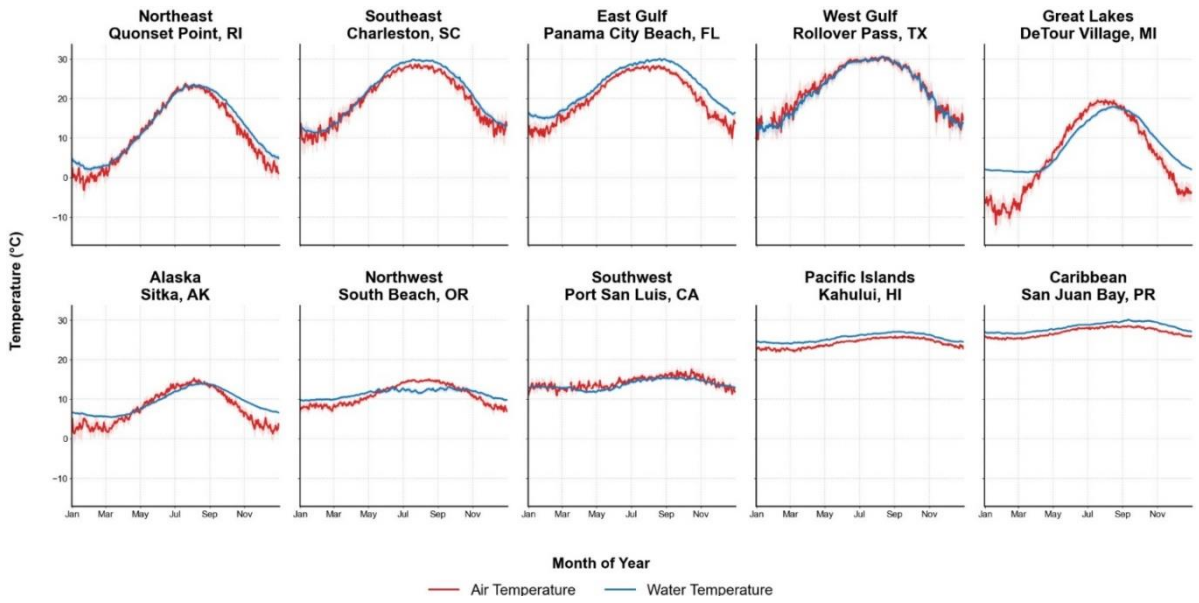

Figure 3. Mean seasonal cycle in coastal water temperature (blue) and air temperature (red) computed from daily climatologies. 95% confidence intervals are shown in shaded areas around each curve.

Along the East and Gulf Coasts, smallest seasonal variations are found in the warmest locations of southeast Florida and the Caribbean Islands, with mean annual ranges of below 10 ℃ and 4 ℃, respectively. Except for the farthest north three stations, all other stations north of FL have relatively similar ranges in the mid to low 20s ℃ (ranging from about 19 to 28 ℃). Gulf coast station ranges are also consistent between approximately 16 - 20 ℃. Small variations in the seasonal cycle are also observed throughout the West Coasts except for slight increases in San Francisco Bay, Toke Point, WA, and Alaska. Other than at Anchorage, AK and Port Chicago, CA, all annual ranges are below 10 ℃, many below 5 ℃. Great Lakes stations have relatively large annual ranges of 17 ℃ to 25 ℃, with minimum temperatures near the freezing mark, as can be seen at DeTour Village, MI in Fig 5.

Stronger seasonal cycles often result in more defined maximum peaks. Applying LOESS (locally estimated scatterplot) smoothing to the seasonal cycles revealed distinct regional variations in peak timing across regions. Stations along the East Coast, Gulf Coast, and the Great Lakes peaked in early August (22–31 ℃), followed by stations along the Northwest and Southwest at the end of the same month (13–18.5 ℃). Alaska also followed a similar mid-August peak (12.5 ℃), while the Caribbean and Pacific Islands reached their thermal maximums latest in the season, peaking in early September with temperatures of 30 ℃ and 28 ℃, respectively. Generally, stations in the higher latitudes stay warm for shorter periods of time, whereas stations in the lower latitudes have relatively consistently warm temperatures for longer periods of time.

Comparison of WT and AT annual ranges shows that ranges in WT are smaller than that of AT at the majority of stations (Figure 4). The largest differences are notably in the Northeast, upper Northwest, Alaska, and Great Lakes regions (Figure S8). For example, stations in Maine have annual ranges of AT and WT of approximately 25 ℃ and 15 ℃, respectively, an average difference of about 14℃ . In contrast, the majority of stations in the Northwest, along the East Coast, and the Island regions have range differences less than 3-4 ℃. Very few stations have slightly larger ranges of WT than AT, primarily in the Southeast and at Alameda, CA, with minor differences less than 2 ℃.

Timing of WT seasonal pattern generally follows AT at nearly all stations except for a few stations in the Southwest and Pacific Islands. Positive values in Figure 4 indicate AT pattern leads WT by the specific noted number of days, on average. Along the East and Gulf Coasts, the largest lags of about 20 days or more are detected at the three Maine stations, New London, CT, and Duck Creek, NC. There was little to no lag along the Southeast, Gulf Coast, and Caribbean stations. Along the West Coast, differences are largest in central to upper northwest and Alaska regions. Largest differences are seen at Port Oxford, OR and Arena Cove, CA, with approximately 90 days lag. These two stations have similar unique annual patterns of WT (Supplemental Figure S9) with very low annual ranges (~ 3 ℃), minimum temperatures extending into June, rising to flattened maximum temperatures spread over the fall.

Comparing the seasonal maximum of WT to MSL revealed that at almost all locations peak WT leads MSL, with few exceptions at Great Lakes stations; Bar Harbor and Portland, ME; Providence, RI, and Charleston, OR (Figure 4). MSL peaks often occur in September/October along the East and Gulf Coast while WT peaks usually occur 1-2 months earlier (Supp Figure S10). The few exceptions are at Vaca Key, FL and Charleston, SC where WT leads MSL by 3 months. Conversely, large differences exist along the West and Alaska Coasts where peak WT leads MSL. In the more northwestern regions, peak MSL occurs in October through January, whereas in the southwestern regions, it occurs in August through October. However, peak WT is relatively consistent along the West Coast, occurring in late summer. For all stations in the Great Lakes, peak WT occurs in late summer and peak MSL usually occurs about 1-2 months later.

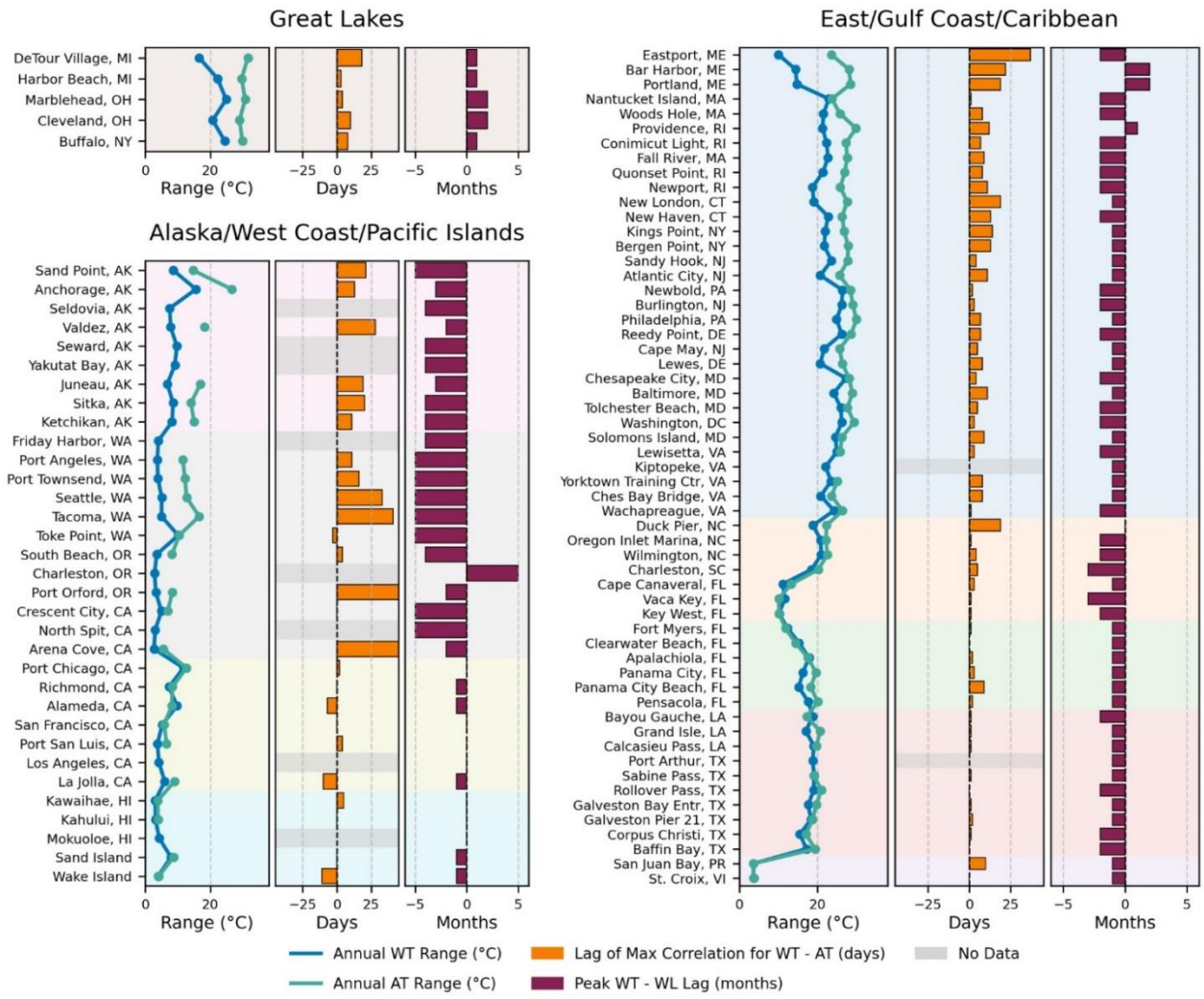

Figure 4. Summary graphic of seasonal variation metrics in coastal water temperature. Background color shades represent different geographic regions (see legend in Figure 6). Annual ranges are maximum minus minimum values from the daily climatology. Days lag between air (AT) and water (WT) temperatures represent the lag that resulted in the maximum correlation between their respective daily climatologies. Positive (Negative) lags denote AT leads (follows) WT. Months lag between WT and mean sea level (MSL) represent the difference between the months with the largest WT and MSL, respectively.

4.2 Daily Distributions

Daily mean WT distributions include a mix of geographically dependent unimodal and bimodal distributions (Figure 5 shows East and West Coasts with additional plots for Gulf Coast, Great Lakes, and Island regions in Supplemental Figure S11). Relatively symmetric, bimodal distributions with wide spread (high standard deviations) are consistently seen along the East Coast with narrower variances in the far north and far south locations. Along the West Coast, Alaska and the upper Northwest show bimodal distributions whereas unimodal distributions are common in the lower Northwest and Southwest. Spreads of the distributions are consistently smaller across the West Coast and high in the Northeast and Great Lakes. Skewness values are near zero, ranging from -0.5 to 0.5, and excess kurtosis is low but consistently negative except for a few West Coast stations, ranging from about 0 to -1.0 (Supplemental Figure S12).

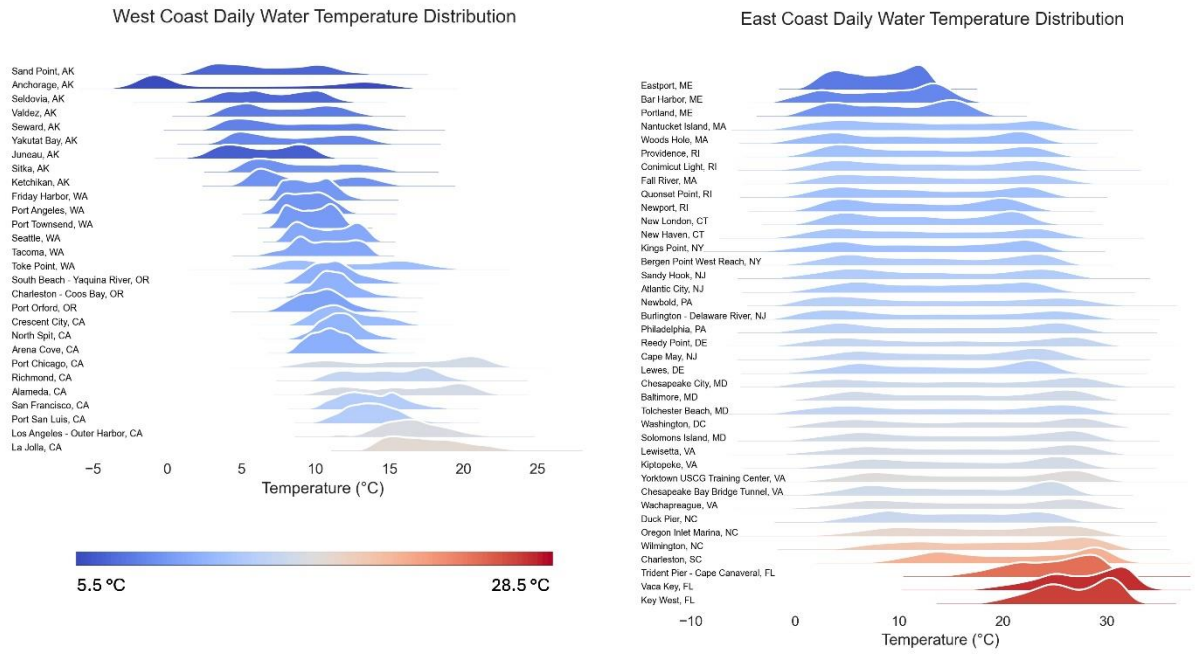

Figure 5. Distributions of daily mean water temperature for the US East and West Coasts. Orientation of stations is generally north to south. Color is based on long-term mean temperature over each stations' POR, scaled over all regions. Distributions for the Gulf, Great Lakes, Pacific islands, and Caribbean regions are shown in Figure S11 in Supplementary Materials.

As expected, lowest mean temperatures are found in Great Lakes and Alaska regions and warmest in the Island regions (Table 2). Smaller standard deviations are found along the West Coast and Island regions, regardless of unimodal or bimodal distribution. The Southeast and both Gulf coasts experience similar characteristics whereas larger differences are seen between Northwest and Southwest regions.

Table 2. Regional mean values of observed daily mean water temperature observations. Values of mean, standard deviation, and extreme percentile levels are in ℃.

Region	Mean	Standard Deviation	90th Percentile	95th Percentile	99th Percentile
Northeast	13.76	7.80	24.00	24.98	26.37
Southeast	21.90	5.70	29.02	29.80	31.14
East Gulf	23.64	5.68	30.49	31.12	32.26
West Gulf	23.13	6.48	30.75	31.43	33.21
Caribbean	28.37	1.39	30.05	30.47	31.41
Great Lakes	11.00	8.04	22.07	23.11	24.42
Alaska	7.68	3.36	12.27	12.92	13.96
Northwest	10.88	1.77	13.23	13.80	14.86
Southwest	15.56	2.67	18.96	19.67	21.03
Pacific Islands	25.93	1.83	28.23	28.65	29.58

Note that for both the unimodal and bimodal distributions of daily WT, the distributions of daily anomalies are much more commonly exhibit near Normal distribution characteristics. Water temperatures tend to stay longer in their warm (June - September) and cold (December - March) phases than during the transition times (Shearman and Lentz, 2010). For example, Newport, RI has a strongly bimodal distribution (with peaks at 5 ℃ and 20 ℃) of daily observations, however, after subtracting out the monthly climatology, the resulting distribution is smooth and near-Normal (Supplemental Figure S14). Based on the Anderson-Darling test, none of the station's daily anomaly distributions were statistically significantly different from Normal at the 0.05 level.

Extreme percentile WTs and anomalies are localized with variation of a few degrees from station to station but do exhibit some general geographic trend (Figure 6). Along both the East and Gulf Coasts, extremes increase gradually from north (cold) to south (warm), with the 99th percentile topping out at approximately 35 ℃. There are only minor differences between the 90th and 95th percentiles at nearly all locations. Slightly larger differences are found between the 95th and 99th percentiles, more noticeably along the East and Gulf coasts, the largest of which are 3-4 ℃ in the Western Gulf, with minimal differences in the Island regions. Extremes of the daily WT anomalies range from 0.62 to 3.4 ℃, 0.83 to 4.3 ℃, and 1.2 to 6.9 ℃, at the 90th, 95th, and 99th percentiles, respectively. The Caribbean and Pacific Island coasts, the two warmest regions, experience the lowest extreme anomalies, whereas the highest extreme anomalies and largest jumps from 95th to 99th percentiles are found in the Gulf regions, indicating higher likelihoods of significant extreme events there. Stations in only two states, Texas (4 stations) and North Carolina (2 stations) make up the top 6 stations with the highest 99th percentile anomalies.

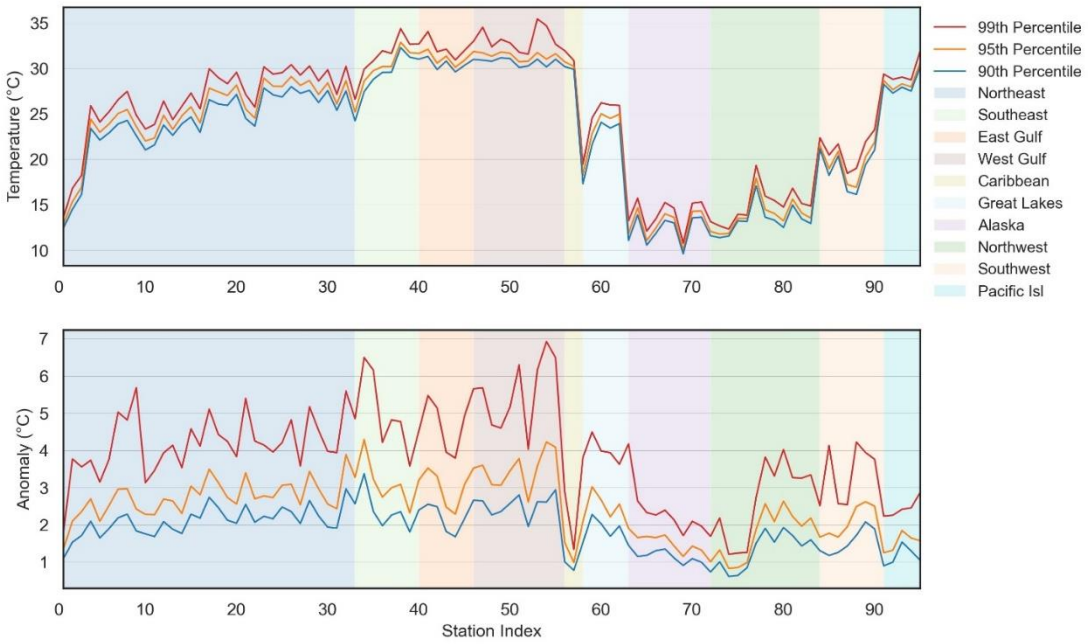

Figure 6. Extreme percentiles thresholds of daily mean water temperature (top panel) and their anomalies from the long-term monthly mean (bottom panel). Values based on KDE-based empirical distributions. Shaded areas represent geographic regions.

4.3 Linear Trends

Linear trend rates are positive at the great majority of stations, indicating a gradual warming over the past few decades. The average trend across all stations is 0.30 ℃ / decade. For comparison, the current global mean SST linear trend rate over the past 30 years is 0.15 ℃ / decade (Samset et al., 2023.) Of the 95 stations, 56 and 48 stations have statistically significant positive trends at the 0.10 and 0.05 levels, respectively. The 90% confidence interval widths range from 0.21 ℃ to 1.66 ℃, sometimes larger than the trend value itself. Durbin-Watson tests showed no evidence that serial correlation exists in the remaining residuals (test statistics ranged from 1.6-2.4). Ljung-Box tests also did not show evidence of serial correlation in the residuals at 84 of the 95 stations.

Highest trend rates are generally found along the East and Gulf Coasts, with 50%-70% of the stations in these regions having statistically significant positive trends. The largest regional mean is in the Southeast at 0.49 ℃ / decade (Supplemental Table S3). Smaller in magnitude but statistically significant trends are observed at 11 of the 12 stations are located in the Southwest and Pacific Island regions. Along the Alaska Coast, 5 of the 9 stations have statistically significant trends with an average rate of 0.20 ℃ / decade. Conversely, the Northwest has the smallest regional mean trend at only 0.03 ℃ / decade and no stations (out of 12) with statistically significant trends. Confidence intervals along the East and Gulf Coasts and Great Lakes are generally larger than those along the West Coast and Island regions. Tacoma, WA is an exception to this with a very large confidence interval of 1.35 ℃ / decade due to significant interannual variability. Linear trends in annual maxima and minima show similar large scale geographic patterns (Supplemental Figure S17). One notable aspect is that in the Southeast and Gulf regions, the annual minima have higher positive trend rates than annual maxima, resulting in a gradual decrease in the annual range. Port Arthur and Baffin Bay showed the largest negative trend in annual maximum likely due to the beginning of the data records coinciding with the extreme warm surface waters in the Gulf in the 2008-2010 time period (NASA GSFC 2009).

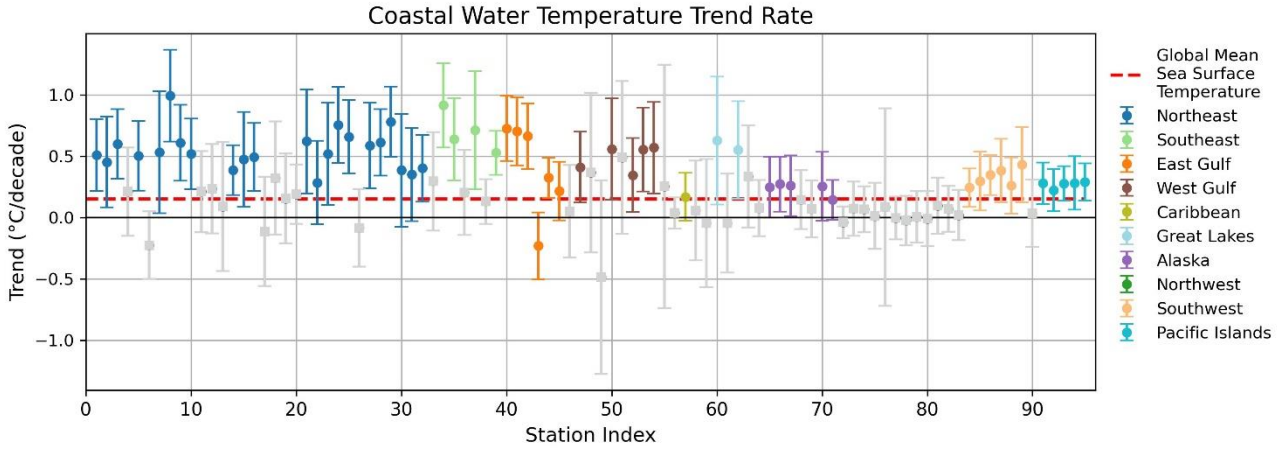

Figure 7. Liner trend rates and 90% confidence intervals of water temperature over each station's POR. Colors represent the geographic region. Data plotted in gray represent trends that are not statistically significant at the 0.10 level. Values are in ℃ / decade.

Two stations stand out as potential outliers from their regional neighbors. Fall River, MA, at 0.99 ℃ / decade, is larger than other stations in the Narragansett Bay, although all stations there show statistically significant trends of approximately 0.5 ℃ / decade. Port Arthur, TX, at -0.49 ℃ / decade, is the only station with a statistically significant negative trend, yet all nearby stations in LA and TX have statistically significant positive trends. Initial review of these stations shows anomalously

elevated values at Fall River at the end of its data record and at Port Arthur at the beginning of its data record, suggesting monitoring or data issues that were missed during the QC procedures in Armos et al. (2025). QC procedures on CO-OPS data records at these stations, as well as at all stations, are continuously being evaluated.

Trends by each month show how the seasons are warming or cooling. Along the East Coast, most months show a positive (warming) trend, aligning the moderately positive long term trends in Figure 7. Cursory analysis showed no single month or season showed much higher rates than the others in most areas. Along the Southeast and Gulf coasts, summer months showed a more negative trend, likely due to anomalously high SSTs in the region in the earlier parts of their data records rather than cool SSTs in recent years; winter months showed stronger positive trends, likely due to high SSTs in later years. Great Lakes stations also show large differences in trends rates across the seasons. Although several stations there show smaller positive or negative trends in the late winter to early spring months, and larger positive trends in the fall to early winter months, no single pattern is consistent throughout the subset of stations in the region.

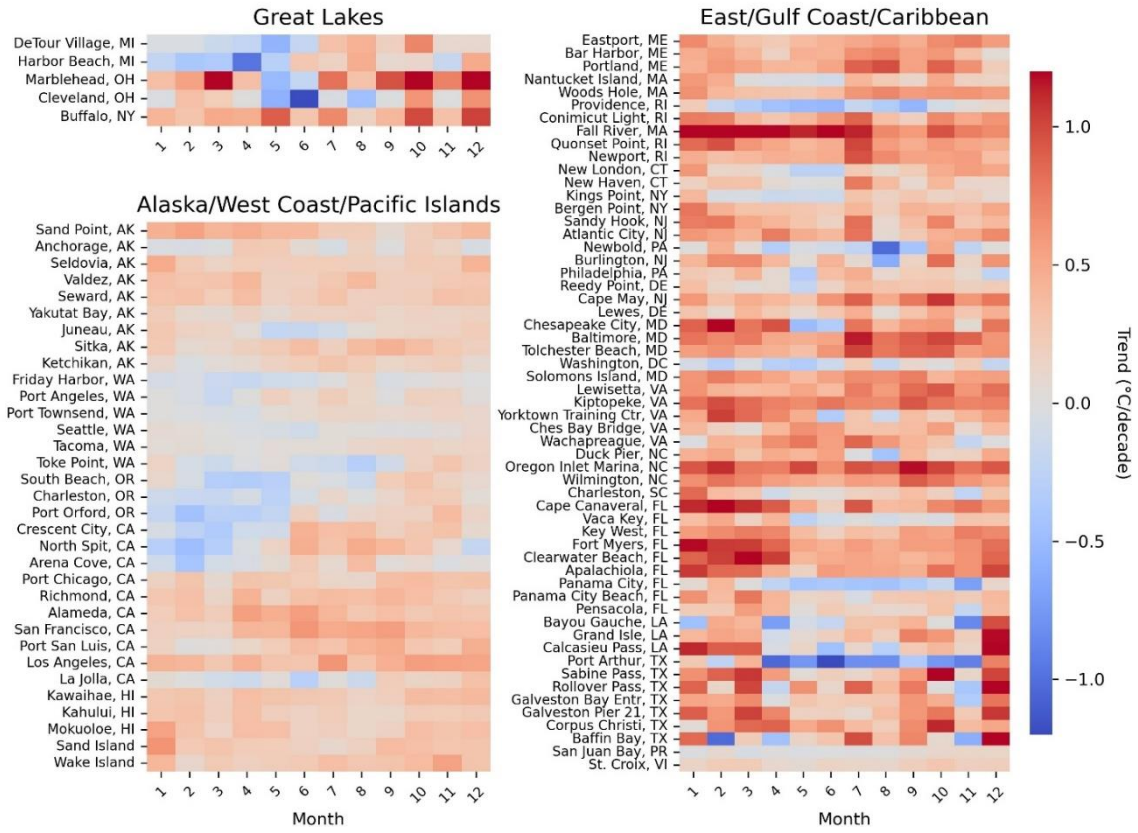

Figure 8. Linear trend rates of water temperature for each month over each station's POR. Values are 974 in °C / decade

West Coast and Island regions show a much smaller seasonal variation in trends than the East and Gulf Coast, consistent with seasonal patterns described above in Section 4.1. With a few exceptions (e.g., Anchorage, AK; La Jolla, CA), locations in Alaska, Southwest, Islands show consistent positive trends throughout the year. Northwest stations, from Arena Cove, CA to Friday Harbor, WA), show a distinct negative trend in the mid-winter to late Spring months, with more positive trends occurring later in the year.

4.4 Case Study 1. OISST Trends in North Carolina

The OISST dataset is globally gridded at 0.25-degree resolution of daily SST observations from 1979 to present (Huang et al. 2020). It incorporates observations from satellites, ships, buoys and Argo floats, offering an independent source of WT data from the CO-OPS stations. Satellite and ship observations are referenced to buoys to compensate for platform differences and sensor biases (Banzon et al., 2016; Huang et al., 2020). Time-series data from OISST Version 2.1[2] were obtained and the hydrologically closest grid point to each station was used for comparison.

Linear trends of WT at the CO-OPS stations and at the nearest OISST grid cell followed very similar patterns across coastal regions (Figure 9). Trend rates are highest in both datasets in the Northeast and lowest in the Northwest, with moderate positive rates in the Gulf, Caribbean, Great Lakes, Alaska, and Southwest coasts. Generally, OISST rates were consistently albeit modestly higher than station rates in the Northeast, Caribbean, and Great Lakes, and lower than station rates in the Gulf Coast and Southwest. The most notable difference is in the Southeast, where the fastest warming station rates are occurring yet OISST shows a cooling negative rate.

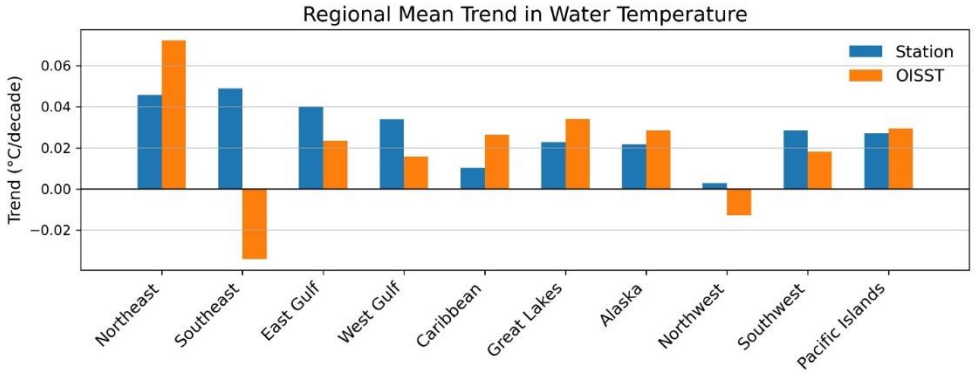

Figure 9. Regional mean WT station-based and OISST-based trend rates. Data are in ℃ / decade.

Station based trend rates within the Southeast were consistent, with statistically significant rates ranging from 0.5 - 0.9 ℃ / decade (Figure 7). However, OISST based rates (Supplemental Figure S20) showed significant negative departures at a couple of stations in North Carolina, namely 8658120 Wilmington and 8652587 Oregon Inlet Marina. At these two locations, from approximately 2008 to present, there is very close agreement between station and OISST datasets. Whereas before that time, OISST showed anomalously warm winter months (Figure 10 shows WIlmington, NC), resulting in a net cooling rate. The issue likely occurred in the data assimilation sources or spatial interpolation algorithms of OISST at that time (NCEI, personal communication). OISST methods have been updated since (Huang, et al, 2021) but not applied retroactively to earlier data. Maps of OISST fields for Dec 1995 and Dec 2015 as an example in Supplemental Figure S19. The Dec 2015 map depicts warmer offshore temperatures in later years, consistent with known ocean warming, yet cooler temperatures very close to shore.

[2] https://www.ncei.noaa.gov/products/optimum-interpolation-sst

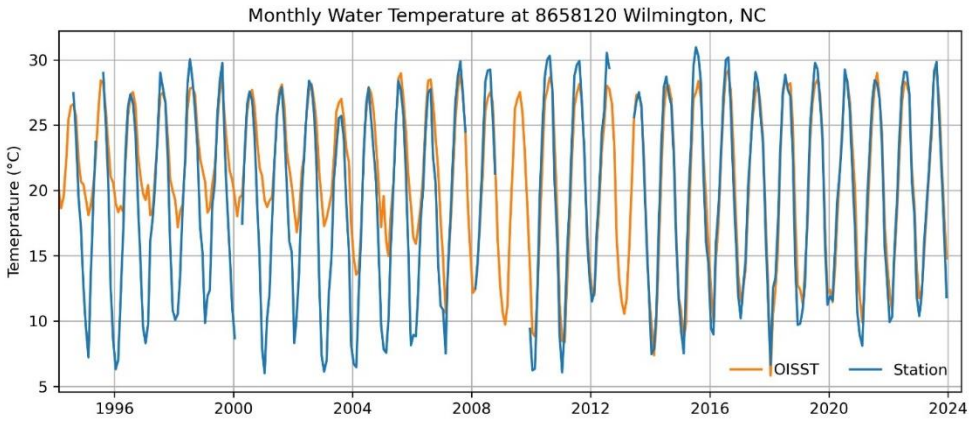

Figure 10. Monthly mean WT at 8658120 Wilmington, NC station and its nearest OISST grid cell. Data in ℃.

4.5 Case Study 2. Marine heat waves and ecosystem stress in South Florida

The Florida Keys represent the northernmost extent of Caribbean reef development, a region increasingly defined by anomalously high water temperatures. At the Key West, FL station (8724580), the 90th percentile threshold for a MHW, calculated via a KDE-based empirical distribution, is established at 30.24°C. Throughout the available historical record (noting a data gap over 2018–2019), every year has experienced at least one MHW event lasting five days or more (Figure 11). While some early years like 1997 and 2000 recorded only a single event, the station reached a historical peak in frequency in 1998 and 2016 with 6 distinct events each. The frequency shows interannual variability fluctuating between two and five events annually (Figure 11).

The most significant shift is observed in the duration of the MHWs. For most of the early record, maximum MHW durations typically remain below 40 days. This baseline was first crossed in 2014 and 2015, which saw events lasting 72 and 90 days. 2023 marked a return to extreme persistence with a maximum duration of also 90 days representing a nearly four time increase over the durations seen in the late 1990s. These primary peaks both in frequency (1998, 2016) and duration (2015, 2023) coincide with strong El Niño events (NOAA CPC 2026), suggesting that ENSO acts as a significant forcing mechanism that amplifies localized thermal stress in the Florida Keys.

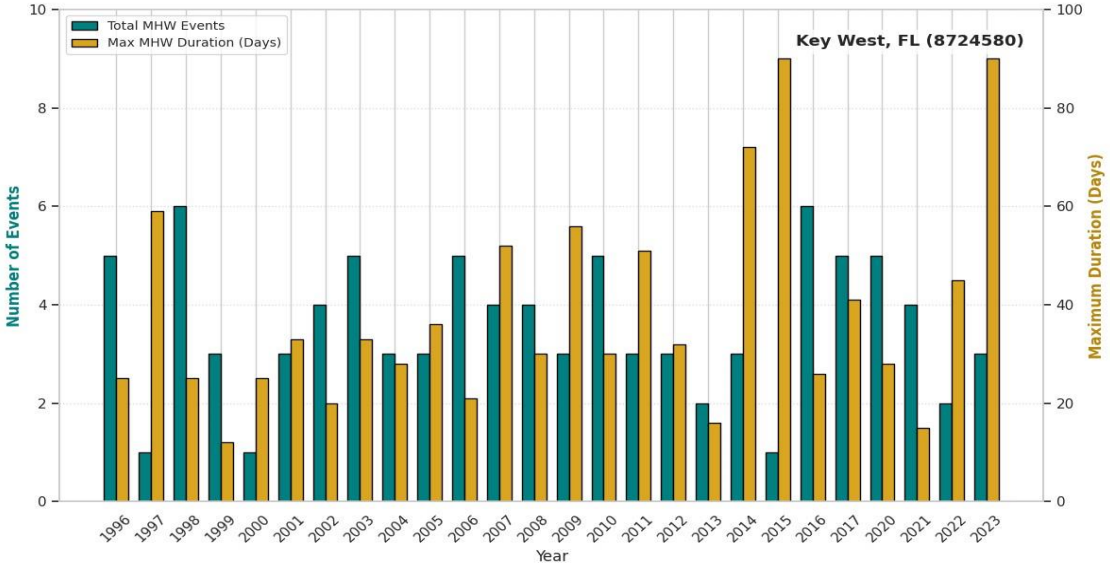

Figure 11. Annual frequency and duration of marine heatwave events at Key West, FL (8724580). The MHW threshold was established at 30.24°C, representing the 90th percentile derived from a KDE-based empirical distribution of daily mean water temperatures over the station's period of record (1996–2023). Note the data gaps for 2018–2019 and the 90-day event duration observed in 2015 and 2023.

A closer analysis of 2023 (Figure 12) reveals an initial MHW event emerged in late May, followed by a brief reprieve where temperatures dipped just below the 90th percentile threshold. Conditions surged again in early June, initiating a massive heatwave that persisted through late August. Following a temporary one-month cooling period, a third distinct MHW emerged in September. These observations align with the NOAA Coral Reef Watch, which issued a coral bleaching warning on June 14th that remained active through September 30th (Neely et al. 2024). Ultimately, these combined heatwaves (especially the second) were the most severe on record for Florida's Coral Reef and the resulting cumulative heat stress led to the widespread coral bleaching and significant mortality documented across the region (Neely et al. 2024; Ayad et al. 2025).

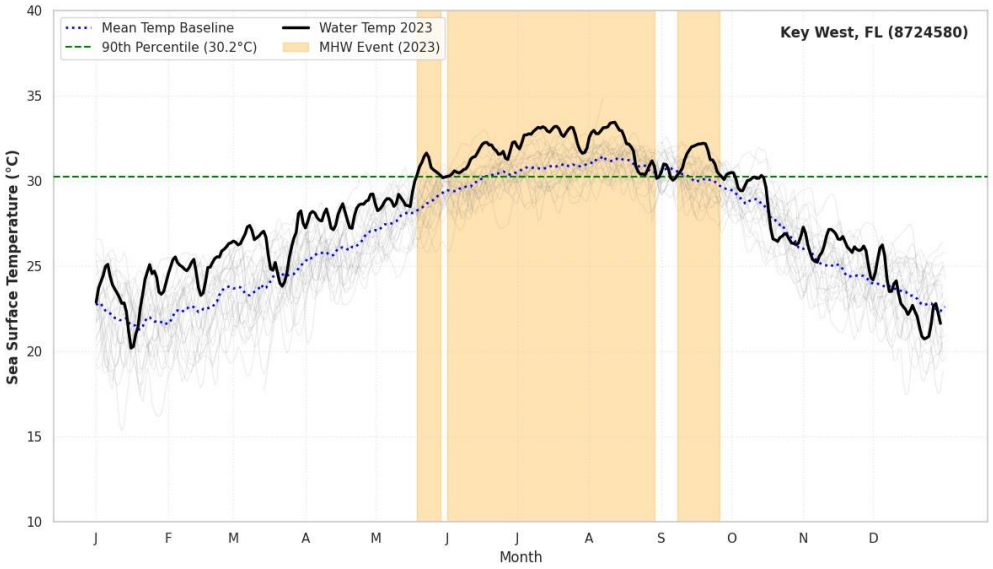

Figure 12. Daily water temperature at Key West, FL with 2023 highlighted black, the mean temperature baseline highlighted blue, and 90% threshold in green. The three MHW event periods are highlighted yellow.

5 Discussion

This paper evaluated seasonal patterns and trends of coastal water temperature data collected at NOAA CO-OPS water level monitoring stations. It builds on QC procedures presented in Armos, et al. (2025) applied to historical daily mean WT data records at 95 stations from 1992 to 2023. Several commonly used metrics were computed for this new WT dataset, such as the daily and monthly climatologies, comparison of the mean seasonal cycle to air temperature and mean sea level, distributions of daily mean WT, estimation of extreme temperature event thresholds, and linear trends over each station's period of record. Two applications of these data were also performed to demonstrate the usefulness of these data: 1) comparison of linear trends in North Carolina to the commonly used NOAA OISST gridded dataset, an independent commonly used source of WT that

extends to the coast, and 2) computation of marine heatwave frequency and accumulated ecosystem stress at Key West, FL. Evaluation of *in situ* observational datasets is critical as large scale, consistent, coastal water temperature datasets are rare, yet they serve to calibrate models or remotely sensed data, and provide a baseline for future changes in complex and highly localized coastal physical environments.

Seasonal cycles of WT are exhibited at nearly all stations, and consistent with geographic regions.. Larger variations in seasonal cycle (stronger seasonality) are seen along the East Coasts as compared to West Coasts, and northern regions as compared to southern regions. Peaks in WT match the seasonal cycle of air temperature, peaking in late summer, The confidence intervals around WT daily climatology are minimal, less than that is air temperature (Figure 3). As well, WT has less variation in the daily climatologies and smaller annual range than AT and less variation in southern latitudes than northern latitudes. Largest differences between the annual ranges in AT and WT are in the coldest regions.

WT seasonality tracks well with solar heating cycle lagging in time by a few days to a few weeks at all coasts, indicating a strong contribution from air-sea exchange of heat rather than ocean factors, most notably in the Great Lakes and least in Island locations. The Loop current in the Gulf brings in warm water from the Caribbean year round, decreasing the contrast between the seasons, resulting in Gulf Coast seasonal cycles not as pronounced as locations further north. The Gulf waters are also typically highly stratified, allowing for air-sea heat exchange near the surface. Daily distributions of the Great Lakes and Gulf Coasts are very similar, mixed bimodal with higher frequency of temperatures in the cold peak in Great Lakes and warm peak in the Gulf stations. In general, the strong seasonal cycles and bimodal distributions show longer periods of time spent around warm and cold periods than in the transition periods, evidence of high persistence and lower high frequency variability in WT.

In contrast to the stations in central FL and northward, stations in the southern portions of FL, from Cape Canaveral to Fort Myers, and the Caribbean all have very small seasonal cycles. Warm waters from the equatorial Atlantic via the Loop Current keep waters warm all year (Figures 3 and S7). Similarly, stations in the Gulf Maine show minimal seasonal cycle, where the Labrador Current is a cooling influence against the warmer waters of the Gulf Stream, keeping the deeper Gulf of Maine waters cool and direct surface heat exchange with the cold atmospheric and high winds (Xue et al., 2000; Seidov et al., 2021).

Along the West Coast, seasonal cycles are often driven by the California Current and seasonal upwelling caused by generally northerly winds, particularly in the Northwest (Jacox et al., 2018). This keeps the near coastal waters cooler in summer than they would be from solar heating alone. Further south, upwelling is less intense and solar heating seasonal contrast is also less, keeping similar annual ranges along the coast. Stations within the two large bay systems show opposite behavior; stations within the Puget Sound have a small seasonal range whereas stations within the San Francisco Bay have a larger seasonal range, showing more evidence on the role of coastal currents.

East and Gulf Coast locations also had higher and more variable extremes than the West Coast. Stations that were the highest peaks were generally those in more enclosed locations or within river estuary systems, like Baffin Bay, TX, Oregon Marina Inlet, NC, and Wilmington, NC all listed in the top 10 daily anomalies seen in Table 3. However, there were also systems, like the San Francisco Bay, that had wide variability within its environment. The southern regions along both

coasts of the continuous US had relatively higher extremes but the warmest stations within the Pacific and Caribbean Islands and the coldest stations in Alaska both have the smallest extremes. This hints at a potential role of CONUS extratropical weather systems playing a large role in the extreme events, which can push warm waters off the coast into the semi-enclosed regions.

Table 3. Top 10 water temperature anomaly events at CO-OPS stations. Anomaly values are referenced to monthly climatology.

Rank	**Station**	**Date**	**Temperature (**℃)	**Anomaly (**℃)
1.	Rollover Pass, TX	2022-01-01	23.24	10.54
2.	Wachapreague, VA	2012-03-24	19.85	10.24
3.	Newbold, PA	2012-03-24	16.31	10.00
4.	Wilmington, NC	2016-01-01	18.56	9.91
5.	Oregon Inlet Marina, NC	2017-04-30	25.48	9.83
6.	Sabine Pass, TX	2009-02-28	24.59	9.82
7.	Oregon Inlet Marina, NC	2022-01-02	17.65	9.65
8.	Wachapreague, VA	2012-03-23	19.24	9.63
9.	Burlington, NJ	2012-03-26	15.40	9.62
10.	Washington, DC	2012-03-24	17.99	9.52

For most locations, water temperatures have been increasing (warming) over the past few decades. A little over half of the stations had statistically significant trends, while most of the remaining stations still showed positive trends although large interannual variation, short PORs, or weak trends prevented statistical significance, which will likely be reached at most locations as data records are extended. There is also some seasonality to WT trends although not as strong as other metrics, indicating the warming forcing is widespread over time and space. For Cape Hatteras and north, trends were slightly higher during the summer months, whereas to the south, trends were slightly higher during the colder months. One mechanism for this difference is that north of Cape Hatteras, the mean coastal current (originating from Labrador Sea) and along shore transport are primarily responsible for long term change whereas southward, the primarily mechanism is atmospheric air-sea exchange of heat (Shearman and Lentz, 2010). At several Northwest and Great Lakes locations we do see some smaller or negative trends in the colder seasons. Port Arthur, TX, Panama City, FL, Newbold, PA, Providence, RI show anomalous cooling in the summer months and need to be investigated further.

Continued increases in the mean temperatures will likely result in increases in the frequency and duration of extreme events above select thresholds, such as marine heatwaves as demonstrated in the Key West, FL case study, exacerbating the impacts of the gradual warming. This is analogous to the observed increases in High-Tide Flooding events due to mean sea level rise; in those cases, increases in flooding events are occurring much faster than mean sea levels (Sweet et al., 2018, 2022).

The record breaking MHW in the Florida Keys was part of a broader global phenomenon. During the summers of 2023-2024, the global average of MHW days was 240% higher than any other year on record, fueled by long-term SST warming and further amplified by El Nino conditions and record low global cloud cover (Smith et al., 2025). Within this context, the MHW event in the Gulf of America that encompassed the Florida Keys was primed by warmer than average ocean surface waters during the winter of 2022. These temperatures were intensified by the extreme exposure to summer solar radiation in 2023. Because the summer solar forcing was so high, standard cooling processes such as vertical mixing were unable to counteract the warming effects, leading to unprecedented thermal persistence in the region (Bailey et al., 2025).

From a hazard perspective, some areas are vulnerable to warming and sea level rise. Areas along the Southeast and Gulf Coasts as well as a few individual stations in the Northeast and Wests Coasts, are undergoing sea level rise, increasing temperatures, and experience regionally high (relative to their neighbors) extreme warming levels (i.e., MHWs). Pearson correlation between linear trend rates of WT to MSL is 0.30 across all stations (Figure 8). Excluding Alaska stations (due to their large positive VLM rates (Sweet et al, 2022)) and Great Lakes stations (due to very different mechanisms driving sea level change) correlation increases to 0.44. Keeping within each region, Alaska and Great Lakes had correlations of 0.45 and -0.57, respectively. Other than the Caribbean with only two stations, the Southeast, an area experiencing high rates of SLR, has the highest correlation of 0.52. Interestingly, the Western Gulf had a low correlation of WT to MSL trends of 0.13, however, when the high rates of VLM (Sweet et al., 2022) are subtracted from MSL rates, the correlation goes up to 0.97. Warming waters and rising sea levels accompany inland flooding, landuse changes, and human development impacting the combined Southeast and Gulf areas (Hoffman et al., 2023).

Seasonally, most station's highest MSL months follow peaks in WT. MSL along the East Coast commonly have two peaks, first in late summer to mid Fall, which consistently lags behind WT peaks by 1-3 months, and a second in mid to late spring. These MSL peaks are due to multiple processes, such as thermal heating, seasonal cycle of atmospheric pressure and ocean currents, and coastal storm development (particularly spring peaks in extratropical systems in the Northeast and Mid-Atlantic, fall peaks in tropical systems in the Southeast and Gulf (Domingues et al., 2018; NOAA, 2021. Hochet et al., 2024; Yan and Chen, 2025). The West Coast was split, with MSL peaks aligning with solar heating patterns in northern CA and southward, and Northwest and Alaska regions with MSL peaks in the winter corresponding to extratropical storms and atmospheric pressure and wind patterns.

Comparing the station observations to OISST data highlights the importance of local *in situ* observations in the shallow water, near coastal regions. Issues with long-term analysis at the two North Carolina stations were described in the case study. Figure 9 also shows that the Northeast has a much larger positive trend in OISST than at the stations. This was due to OISST higher positive rates in the Chesapeake Bay. Additionally (not shown), based on f-tests of the residuals after detrending and deseasonalizing, about 75% of the stations tested exhibited statistically significant differences between the two datasets. OISST is a valuable dataset to estimate large scale estimates of SSTs and combines multiple types of data sources. However, the final OISST product is subject to the quantity and density of assimilated observations, which change over time, and its interpolation algorithms, which may not be representative of near shore locations.

A few stations stand out as potential outliers from their neighbors. While the largest positive trend was recorded at Fall River, MA, at 1.0 ℃ / decade, subsequent review reveals this may be due to anomalous elevated values toward the end of the data record. At Panama City, FL and Port Arthur,

TX, metadata analysis indicated initial deployments yielded slightly elevated temperatures at the beginning of the record, creating an artificial downward slope rather than cooling over time, despite no recorded changes in sensor depth. Although a significant amount of QC was performed in Armos et al. (2025), data records are continuously being evaluated by the authors.

The statistics computed in this study were simple commonly used metrics. Although this was intentional to compare this new dataset to other WT datasets, and to provide a baseline for future studies as WT station records increase, deeper investigations may lead to different results on the applicability of these data in specific contexts. Similarly, the length of the PORs (~20-30 years) is relatively short to provide high confidence on past linear trends. Typical lengths of computing climate normals of air temperature is 30 years, assumed to be long enough to minimize the influence of interannual variability. Longer time frame and/or higher order trends may refine the rate of change or narrow the confidence. This study did not evaluate periodicity in the WT time series record or correlations with large scale weather patterns (i.e., ENSO and PDO climate oscillations). Further planned investigations will focus on driving factors influencing low-frequency WT changes at interannual or decadal time scales.

The new dataset emphasizes the importance of local *in situ* observations in detecting past changes. Monitoring in complex coastal areas is critical in assessing the health of our coastal resources and how they can support the health and safety of US citizens, its economy, and its natural resources. Coastal intelligence that supports evidence-based decisions to address critical societal challenges, including energy security, food and water availability, and economic prosperity are obtained from observations (Bailey et al., 2019).

These data, along with other coastal observations collected by NOAA and other federal agencies, are available for federal and state government agencies, non-profit and private sectors, local communities, academic users, and to the public, for research, education, or decision making. This study will hopefully contribute to the research and development of coastal water temperature data products that will enrich continued coastal resilience information for safety and preparedness of the nation.

Acknowledgments

Many individuals contributed to the development of the data used in this study. The authors would like to thank the CO-OPS Field Operations Division for instrument installation and maintenance; the Engineering Division for instrumentation testing, calibration, metadata management and data transmission; Continuous Operational Real-Time Monitoring System (CORMS) group for real-time processing the data; and the Information Systems Division for data ingestion and storage. Authors would also like to thank several internal and external reviewers of the manuscript. These reviews improved the content and clarity of the manuscript and graphics.

References

Aroucha, L. C., Lübbecke, J. F., Brandt, B. Schwarzkopf, F. U. and Biastoch, A. (2025). River discharge impacts coastal southeastern tropical Atlantic sea surface temperature and circulation: a model-based analysis.*Ocean Science*, Volume 21, issue 2. https://doi.org/10.5194/os-21-661-2025

Armos, Bailey, Tigist Jima, Chris Zervas, and John A. Callahan (2025). Evaluation and Quality Control of CO-OPS Coastal Water Temperature Data. NOAA Technical Report NOS CO-OPS 114. 92 pp. https://doi.org/10.25923/n65z-p624

Ayad, Mariam et al. "Impacts of the 2023 Marine Heatwave in the Florida Keys: Detection and Analysis of a Mass Coral Bleaching Event Using Spaceborne Remote Sensing Imagery." *Environmental science & technology* vol. 59,29 (2025): 15227-15235. https://doi.org/10.1021/acs.est.5c03122

Bailey K, Steinberg C, Davies C, Galibert G, Hidas M, McManus MA, Murphy T, Newton J, Roughan M and Schaeffer A (2019) Coastal Mooring Observing Networks and Their Data Products: Recommendations for the Next Decade. *Frontiers in Marine Science* 6:180. http://doi.org/10.3389/fmars.2019.00180

Bailey, S. T., Drake, H. F., Gruenburg, L. K., Abernathey, R. P., & Torres, M. I. (2025) The thermodynamics of the 2023 Gulf of Mexico Marine heatwave. Geophysical Research Letters, 52, e2024GL111768. https://doi.org/10.1029/2024GL111768

Bamston, A. G., Chelliah, M., and Goldenberg, S. B. (1997). Documentation of a highly ENSO-related SST region in the equatorial pacific: Research note. Atmosphere-Ocean, 35(3), 367–383. https://doi.org/10.1080/07055900.1997.9649597

Bashevkin, S.M., Mahardja, B. and Brown, L.R. (2022). Warming in the upper San Francisco Estuary: Patterns of water temperature change from five decades of data, Limnology and Oceanography, 67(5), pp. 1065-1080. doi: 10.1002/lno.120571

Cooley, S., D. Schoeman, L. Bopp, P. Boyd, S. Donner, D.Y. Ghebrehiwet, S.-I. Ito, W. Kiessling, P. Martinetto, E. Ojea, M.-F. Racault, B. Rost, and M. Skern-Mauritzen (2022). Oceans and Coastal Ecosystems and Their Services. In: Climate Change 2022: Impacts, Adaptation and Vulnerability. Contribution of Working Group II to the Sixth Assessment Report of the Intergovernmental Panel on Climate Change [H.-O. Pörtner, D.C. Roberts, M. Tignor, E.S. Poloczanska, K. Mintenbeck, A. Alegría, M. Craig, S. Langsdorf, S. Löschke, V. Möller, A. Okem, B. Rama (eds.)]. Cambridge University Press, Cambridge, UK and New York, NY, USA, pp. 379–550, doi:10.1017/9781009325844.005.

Domingues, R., Goni, G., Baringer, M., & Volkov, D. (2018). What caused the accelerated sea level changes along the U.S. East Coast during 2010–2015?Geophysical Research Letters, 45, 13,367–13,376. https://doi.org/10.1029/2018GL081183

Dusek, G., Loesch, R., Stone, P., Heilman, L., and Fiorentino, L. (2024). National Water Level Observation Network (NWLON) Requirement. *NOAA Technical Report NOS CO-OPS 107*. https://doi.org/10.25923/h9h9-6p20

Edwing, R. F. (1991) Next Generation Water Level Measurement System (NGWLS) Site Design, Preparation, and Installation Manual. U.S. Department of Commerce, National Oceanic and Atmospheric Administration, National Ocean Service, Office of Oceanography and Marine Assessment, pp 80. https://tidesandcurrents.noaa.gov/fieldlibrary/ViewLibrary?q=3.2.3.1.A1_

Ezer, T., Dangendorf, S. (2022). The impact of remote temperature anomalies on the strength and position of the Gulf Stream and on coastal sea level variability: a model sensitivity study. *Ocean Dynamics* 72, 223–239. https://doi.org/10.1007/s10236-022-01500-4

Fox-Kemper, B., H.T. Hewitt, C. Xiao, G. Aðalgeirsdóttir, S.S. Drijfhout, T.L. Edwards, N.R. Golledge, M. Hemer, R.E. Kopp, G. Krinner, A. Mix, D. Notz, S. Nowicki, I.S. Nurhati, L. Ruiz, J.-B. Sallée, A.B.A. Slangen, and Y.

Yu (2021). Ocean, Cryosphere and Sea Level Change. In Climate Change 2021: The Physical Science Basis. Contribution of Working 2025 Delaware Climate Change Projections Group I to the Sixth Assessment Report of the Intergovernmental Panel on Climate Change [Masson-Delmotte, V., P. Zhai, A. Pirani, S.L. Connors, C. Péan, S. Berger, N. Caud, Y. Chen, L. Goldfarb, M.I. Gomis, M. Huang, K. Leitzell, E. Lonnoy, J.B.R. Matthews, T.K. Maycock, T. Waterfield, O. Yelekçi, R. Yu, and B. Zhou (eds.)]. Cambridge University Press, Cambridge, United Kingdom and New York, NY, USA, pp. 1211–1362, https://doi.org/10.1017/9781009157896.011

[GMRI] Gulf of Maine Research Institute (2025). 2024 Gulf of Maine Warming Update. https://gmri.org/stories/warming-24. Accessed April 1, 2026.

Goddard, P., Yin, J., Griffies, S. et al. (2015). An extreme event of sea-level rise along the Northeast coast of North America in 2009–2010. Nature Communications, 6, 6346. https://doi.org/10.1038/ncomms7346

Hall, M.O., Furman, B.T., Merello, M., Durako, M.J. (2016). Recurrence of Thalassia testudinum seagrass die-off in Florida Bay, USA: initial observations. *Marine Ecology Progress Series.* 560: 243-249

Hamlington, B.D., C.G. Piecuch, J.T. Reager, H. Chandanpurkar, T. Frederikse, R.S. Nerem, J.T. Fasullo, and S.-H. Cheon (2020). Origin of interannual variability in global mean sea level. *Proceedings of the National Academy of Sciences*, 117 (25), 13983. http://dx.doi.org/10.1073/pnas.1922190117

Hamlington, B.D., Bellas-Manley, A., Willis, J.K. et al. (2024). The rate of global sea level rise doubled during the past three decades. *Commun Earth Environ* 5, 601. https://doi.org/10.1038/s43247-024-01761-5

Heil, C.A., and Muni-Morgan, A.L. (2021). Florida's Harmful Algal Bloom (HAB) Problem: Escalating Risks to Human, Environmental and Economic Health With Climate Change. Front. Ecol. Evol. https://doi.org/10.3389/fevo.2021.646080

Hinson, K.E., M.A.M. Friedrichs, P. St-Laurent, F. Da, and R.G. Najjar (2022). Extent and Causes of Chesapeake Bay Warming. *Journal of the American Water Resources Association,* 58 (6): 805–825. https://doi.org/10.1111/1752-1688.12916.

Hochet, A., Llovel, W., Huck, T. et al. (2025). Advection surface-flux balance controls the seasonal steric sea level amplitude. Sci Rep 14, 10644. https://doi.org/10.1038/s41598-024-61447-y

Hoffman, J.S., S.G. McNulty, C. Brown, K.D. Dello, P.N. Knox, A. Lascurain, C. Mickalonis, G.T. Mitchum, L. Rivers III, M. Schaefer, G.P. Smith, J.S. Camp, and K.M. Wood (2023). Ch. 22. Southeast. In: Fifth National Climate Assessment. Crimmins, A.R., C.W. Avery, D.R. Easterling, K.E. Kunkel, B.C. Stewart, and T.K. Maycock, Eds. U.S. Global Change Research Program, Washington, DC, USA. https://doi.org/10.7930/NCA5.2023.CH22

Huang, B., C. Liu, V. Banzon, E. Freeman, G. Graham, B. Hankins, T. Smith, and H.-M. Zhang (2020). Improvements of the Daily Optimum Interpolation Sea Surface Temperature (DOISST) Version 2.1, Journal of Climate, 34, 2923-2939. doi: 10.1175/JCLI-D-20-0166.1

Jacox, M. G., Edwards, C. A., Hazen, E. L., & Bograd, S. J. (2018). Coastal upwelling revisited: Ekman, Bakun, and improved upwelling indices for the U.S. West Coast. Journal of Geophysical Research: Oceans, 123, 7332–7350. https://doi.org/10.1029/2018JC014187

Liao E, Lu W, Yan XH, Jiang Y, Kidwell A. (2015). The coastal ocean response to the global warming acceleration and hiatus. *Scientific Reports*, Nov 16;5:16630. http://doi.org/10.1038/srep16630.

Lima, F. and Wethey, D. (2012). Three decades of high-resolution coastal sea surface temperatures reveal more than warming. *Nat Commun* 3, 704. https://doi.org/10.1038/ncomms1713

Malone, T.C. and Newton, A. (2020). The Globalization of Cultural Eutrophication in the Coastal Ocean: Causes and Consequences. *Frontiers in Marine.Science*, Vol 7:670. http://doi.org/10.3389/fmars.2020.00670

May, C.L., M.S. Osler, H.F. Stockdon, P.L. Barnard, J.A. Callahan, R.C. Collini, C.M. Ferreira, J. Finzi Hart, E.E. Lentz, T.B. Mahoney, W. Sweet, D. Walker, and C.P. Weaver. (2023): Ch. 9. Coastal effects. In: Fifth National Climate Assessment. Crimmins, A.R., C.W. Avery, D.R. Easterling, K.E. Kunkel, B.C. Stewart, and T.K. Maycock, Eds. U.S. Global Change Research Program, Washington, DC, USA. https://doi.org/10.7930/NCA5.2023.CH9

Miller, A. and Luscher, A. (2019). NOAA's national water level observation network (NWLON). *Journal of Operational Oceanography*, *12*(sup2), S57-S66. https://doi.org/10.1080/1755876X.2018.1523301

[NASA GSFC] NASA Goddard Space Flight Center (2009). 2008 Sea Surface Temperature in the Gulf of Mexico, NASA GSFC Scientific Visualization Studio. https://svs.gsfc.nasa.gov/3397. Accessed April 1, 2026.

Neely, KL, Nowicki, RJ, Dobler, MA, Chaparro, AA, Miller, SM, and Toth, KA (2024). Too hot to handle? The impact of the 2023 marine heatwave on Florida Keys coral. Front. Mar. Sci. 11:1489273. https://doi.org/10.3389/fmars.2024.1489273

NOAA (2021). Interactive map: How has local sea level in the United States changed over time? https://www.climate.gov/news-features/features/interactive-map-how-has-local-sea-level-united-states-changed-over-time. Access February 2, 2026.

NOAA CO-OPS (2025a). NOAA Relative Sea Level Trends, Tides and Currents. https://tidesandcurrents.noaa.gov/sltrends/sltrends.html. Accessed October 16, 2025.

[CPC] NOAA Climate Prediction Center (2025). Oceanic Nino Index (ONI). Data obtained from https://www.cpc.ncep.noaa.gov/products/analysis_monitoring/ensostuff/ONI_v5.php. Accessed May 20, 2025.

[NAMES] NOAA National Marine Ecosystem Status (2026). Marine Heatwaves. https://ecowatch.noaa.gov/thematic/marine-heatwaves. Accessed March 15, 2026.

[NGS] NOAA National Geodetic Survey (2025). *Continually Updated Shoreline Product* [Data set]. NOAA Digital Coast. https://coast.noaa.gov/digitalcoast/data/cusp.html

[NOS] NOAA National Ocean Service, The Center for Operational Oceanographic Products and Services. *NOAA's Coastal Ocean Reanalysis (CORA) Dataset*. https://registry.opendata.aws/noaa-nos-cora/

[NWS] NOAA National Weather Service Instruction 10-1302 (2023). Requirements and Standards for NWS Climate Observations. https://www.weather.gov/directives/010

O'Dnnell, K. L., Bernhardt, E. S., Yang, X. Emanuel, R. E., Ardón, M., Lerdau, M. T., Manda, A. K., Braswell, A. E., BenDor, T. K., Edwards, E. C., Frankenberg, E., Helton, A. M., Kominoski, J. S., Lesen, A. E., Naylor, L., Noe, G., Tully, K. L., White, E., and Wright, J. P. (2024). Saltwater intrusion and sea level rise threatens U.S. rural coastal landscapes and communities. Anthropocene, Volume 45, ISSN 2213-3054. https://doi.org/10.1016/j.ancene.2024.100427.

Parker, B. (2007). *Tidal Analysis and Prediction*. NOAA Special Publication NOS CO-OPS 3.

Qu, J. and Peng, J. (2025). Significance and Enlightenment of Implementing Water Ecological Assessment. W*ater & Ecology,* Volume 1, Issue 1. https://doi.org/10.1016/j.wateco.2025.100002

Reimann, L., Vafeidis, A.T., and Honsel, L.E. (2023). Population development as a driver of coastal risk: Current trends and future pathways. *Cambridge Prisms: Coastal Futures*. https://doi.org/10.1017/cft.2023.3.pr1

Rose, L., Widlansky, M. J., Feng, X., Thompson, P., Asher, T. G., Dusek, G., et al. (2024). Assessment of water levels from 43 years of NOAA's Coastal Ocean Reanalysis (CORA) for the Gulf of Mexico and East Coasts. *Frontiers in Marine Science*, *11*, 1381228. https://doi.org/10.3389/fmars.2024.1381228

Samset, B.H., Zhou, C., Fuglestvedt, J.S., Lund, M.T., Marotzke, J., and Zelinka, M.D. (2023). Steady global surface warming from 1973 to 2022 but increased warming rate after 1990. Commun Earth Environ 4, 400. https://doi.org/10.1038/s43247-023-01061-4

Schemm, S., Castro, L.M., Li, C., Kvamsto, N.G (2016). Influence of Tropical Pacific Sea Surface Temperature on the Genesis of Gulf Stream Cyclones. *Journal of Atmospheric Sciences*, 73(10), 4203-4214. https://doi.org/10.1175/JAS-D-16-0072.1

Seekell, D.A. and Pacea, M. L. (2011). Climate change drives warming in the Hudson River Estuary, New York (USA). Journal of Environmental Monitoring, 11:8. https://doi.org/10.1039/C1EM10053J

Seidov, D., Mishonov, A. and Parsons, R. (2021). Recent warming and decadal variability of Gulf of Maine and Slope Water. Limnol Oceanogr, 66: 3472-3488. https://doi.org/10.1002/lno.11892

Scott, D. W. (1992). "Multivariate Density Estimation: Theory, Practice, and Visualization", John Wiley & Sons, New York, Chichester.

Shearman, R.K. and Lentz, S.J. (2010). Long-Term Sea Surface Temperature Variability along the U.S. East Coast. Journal of Physical Oceanography, Volume 40, 1004–1017. https://doi.org/10.1175/2009JPO4300.1

Shelton A.O., Sullaway G.H., Ward E.J., et al. (2021) Redistribution of salmon populations in the northeast Pacific ocean in response to climate. Fish and Fisheries. 22:503–517. https://doi.org/10.1111/faf.12530

Silva, E., Counillon, F., Brajard, J., Davy, R., Outten, S., Pettersson, L.H., and Keenlyside, N. (2025). Warming and freshening coastal waters impact harmful algal bloom frequency in high latitudes. *Commun Earth Environ* 6, 445. https://doi.org/10.1038/s43247-025-02421-y

Silverman, B. W. (1986). "Density Estimation for Statistics and Data Analysis", Vol. 26, Monographs on Statistics and Applied Probability, Chapman and Hall, London.

Smith, K.E., Sen Gupta, A., Burrows, M.T. *et al.* Ocean extremes as a stress test for marine ecosystems and society. *Nat. Clim. Chang.* 15, 231–235 (2025). https://doi.org/10.1038/s41558-025-02269-2

Sweet, W. V., Dusek, G., Obeysekera, J. T. B., and Marra, J. J. (2018). *Patterns and projections of high tide flooding along the US coastline using a common impact threshold*. NOAA Technical Report NOS CO-OPS 086.

Sweet, W.V., Hamlington, B.D., Kopp, R.E., Weaver, C.P., Barnard, P.L., Bekaert, D., Brooks, W, et al. (2022). *Global and Regional Sea Level Rise Scenarios for the United States: Updated Mean Projections and Extreme Water Level Probabilities Along U.S. Coastlines*. NOAA Technical Report NOS 01.

Tanaka, K.R., Torre, M.P., Saba, V.S., Stock, C.A., Chen, Y. (2020). An ensemble high-resolution projection of changes in the future habitat of American lobster and sea scallop in the Northeast US continental shelf. *Biodiversity Research.* 26:987–1001. https://doi.org/10.1111/ddi.13069

Terhaar, J., Burger, F.A., Vogt, L., Frölicher, T. L. and Stocker, S. T. (2025). Record sea surface temperature jump in 2023–2024 unlikely but not unexpected. Nature 639, 942–946. https://doi.org/10.1038/s41586-025-08674-z

Tester, P.A., Feldman, R.L., Nau, A.W., Kibler, S.R., Litaker ,R.W. (2010). Ciguatera fish poisoning and sea surface temperatures in the Caribbean Sea and the West Indies. Toxicon. 56(5), 698-710. https://doi.org/10.1016/j.toxicon.2010.02.026

Trombetta T, Vidussi F, Mas S, Parin D, Simier M, et al. (2019). Water temperature drives phytoplankton blooms in coastal waters. PLOS ONE 14(4): e0214933. https://doi.org/10.1371/journal.pone.0214933

Tsimplis, M. N. and Woodworth, P. L. (1994). The global distribution of the seasonal sea level cycle calculated from coastal tide gauge data. *Journal of Geophysical Research: Oceans*, *99*(C8), 16031-16039. https://doi.org/10.1029/94JC01115

Varela, R., de Castro, M., Dias, J.M. and Gómez-Gesteira, M. (2023) 'Coastal warming under climate change: Global, faster and heterogeneous', Science of the Total Environment, 886, p. 164029

Wilks, D. S. (2011). *Statistical methods in the atmospheric sciences* (Vol. 100). Academic press.

[WMO] World Meteorological Organization. 2025. State of the Global Climate 2024. Geneva. https://library.wmo.int/idurl/4/69455

Xu, T., Newman, M., Capotondi, A. et al. (2022). An increase in marine heatwaves without significant changes in surface ocean temperature variability. Nat Commun 13, 7396. https://doi.org/10.1038/s41467-022-34934-x

Xue, H., F. Chai, and N. R. Perrigrew. (2000). A model study of the seasonal circulation in the Gulf of Maine. J. Phys. Oceanogr., 30, 1,111-1,134.

Yang, J., & Chen, K. (2025). Profound changes in the seasonal cycle of sea level along the United States Mid-Atlantic Coast. Geophysical Research Letters, 52, e2024GL112273. https://doi.org/10.1029/2024GL112273

Zervas, C. (2009). *Sea level variations in the United States, 1854-2006*. NOAA Technical Report NOS CO-OPS 053.

Zhang, W., Zhao, Z., Hobday, A. J., & Holbrook, N. J. (2026). Projected global diversity of marine heatwaves in the 21st century. Geophysical Research Letters, 53, e2025GL120526. https://doi.org/10.1029/2025GL120526